



Enhancement of room-temperature 2DHG conductivity in narrow and strained double-sides modulation doped Ge quantum well

M. Myronov^{a,c,*}, Y. Shiraki^a, T. Mouri^b, K.M. Itoh^b

^a Research Center for Silicon Nano-Science, Advanced Research Laboratories, Musashi Institute of Technology, 8-15-1 Todoroki, Setagaya-ku, Tokyo 158-0082, Japan

^b Department of Applied Physics and Physico-Imformatics, Keio University, Yokohama 223-8522, Japan

^c Department of Physics, The University of Warwick, Coventry CV4 7AL, UK

ARTICLE INFO

Available online 17 August 2008

Keywords:

Ge quantum well
2DHG
MBE
Mobility

ABSTRACT

Over three times enhancement of room-temperature two-dimensional hole gas (2DHG) conductivity, up to 649.3 μS , by implementation of double-sides modulation doping with strained Ge quantum well (QW) of the same thickness was obtained. The improvement was achieved by successful increase of the 2DHG density due to modification of valence band profile of Ge QW. The obtained 2DHG conductivity exceeds the previously reported high mobility two-dimensional electron gas and 2DHG conductivities.

© 2008 Elsevier B.V. All rights reserved.

The modulation doped heterostructures (MODH) with strained Ge and SiGe quantum wells (QWs) grown on underlying Si(001) substrate via implementation of intermediate relaxed SiGe buffer have been exhibiting significant progress in enhancement of low- and room-temperature two-dimensional hole gas (2DHG) mobilities [1–6]. For high performance Field Effect Transistor (FET) device applications, it is important for the mobile carriers in the channel layer, i.e. QW, not only to have as high mobility as possible but also high conductivity. Conventional Hall effect and resistivity measurements have been widely used to obtain 2DHG mobility and density in a QW at low temperatures in the absence of parallel conduction. Due to activation of carriers in parallel conduction layers of SiGe MODH with the increase of temperature, however, this way of measurements gives an average mobility and carrier density of all conduction layers. In order to find out the transport properties of various carriers existing in multilayer semiconductor heterostructures, the magnetic-field dependence of magnetoresistance and Hall resistance have to be measured and the technique of mobility spectrum analysis (MSA) has to be applied [7].

In this work, over three times enhancement of room-temperature 2DHG conductivity, up to 649.3 μS , was found to be obtained in the 8 nm thick strained Ge QW of Si/Si_{0.32}Ge_{0.68}/Ge/Si_{0.32}Ge_{0.68}/Si_{0.7}Ge_{0.3}/Si(001) *p*-type heterostructure by implementing double-sides modulation doping (DS-MOD) from bottom and top sides of Ge QW compared to that of single-side modulation doping (SS-MOD) structure.

The Si/Si_{0.32}Ge_{0.68}/Ge/Si_{0.32}Ge_{0.68}/Si_{0.7}Ge_{0.3}/Si(001) *p*-type DS-MOD heterostructures were grown on a Si(001) substrate by solid source molecular beam epitaxy. The active region of SiGe heterostructure with symmetric DS-MOD was grown on Si_{0.32}Ge_{0.68}/Si_{0.7}Ge_{0.3}/Si(001) virtual

substrate (VS) consists of a 10 nm Si_{0.32}Ge_{0.68} B-doped supply layer ($\sim 1 \times 10^{18} \text{ cm}^{-3}$), a 10 nm Si_{0.32}Ge_{0.68} undoped spacer layer, a 8 nm undoped Ge QW layer for mobile holes, a 10 nm Si_{0.32}Ge_{0.68} undoped spacer layer, a 10 nm Si_{0.32}Ge_{0.68} B-doped supply layer ($\sim 1 \times 10^{18} \text{ cm}^{-3}$), a 30 nm Si_{0.32}Ge_{0.68} undoped cap layer, and a 2 nm Si cap layer on the surface. The undoped spacer layers separate the ionized B-dopants from the Ge QW. A reference sample of similar design but with single-side modulation doping and an inverted Si_{0.32}Ge_{0.68} B-doped supply layer of $\sim 2 \times 10^{18} \text{ cm}^{-3}$ separated by 20 nm spacer was prepared for comparison. Further details of the samples' structure, growth conditions, electrical and structural characterization can be found elsewhere [8]. The magnetic-field dependence of the magnetoresistance and Hall resistance were measured as the magnetic field was swept continuously from -9 up to $+9$ T and reversed. The measured data were converted into conductivity tensor components followed by a maximum-entropy mobility spectrum analysis (ME-MSA) fitting procedure [7]. It is worth pointing out that the ME-MSA approach does not require any preliminary assumptions about the number of different types of carriers.

Fig. 1 shows the result of ME-MSA fit of magnetic-field dependence of conductivity tensor components, $\sigma_{xx}(B)$ and $\sigma_{xy}(B)$, measured at room temperature for DS-MOD Ge QW heterostructure. The fitted magnetic-field dependencies of $\sigma_{xx}(B)$ and $\sigma_{xy}(B)$ are in very good agreement with the measured ones. The similar results were obtained for SS-MOD Ge QW heterostructure. Fig. 2 shows mobility spectrum as the result of $\sigma_{xx}(B)$ and $\sigma_{xy}(B)$ fits measured at room temperature for DS-MOD Ge QW heterostructure. Obtained mobility spectrum consists of two peaks representing different groups of carriers with specific mobilities associated with 2DHG in the strained Ge QW and parallel conduction layers. Conductivity of the latter one decreases with decreasing temperature due to carriers freeze-out, similar to previously reported data [6]. The conductivity due to each group of carriers was obtained by the integration of the area of each peak in the

* Corresponding author. Present address: Department of Physics, The University of Warwick, Coventry CV4 7AL, UK.

E-mail address: Maksym.Myronov@yahoo.co.uk (M. Myronov).

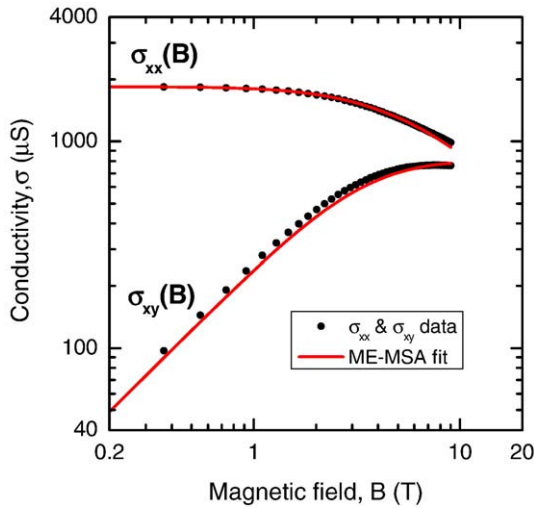


Fig. 1. The ME-MSA fit (solid lines) of magnetic-field dependence of conductivity tensor components, $\sigma_{xx}(B)$ and $\sigma_{xy}(B)$, measured at room temperature (circles) for DS-MOD Ge QW heterostructure.

mobility spectrum. The measured Hall mobility of $1500 \text{ cm}^2 \text{ V}^{-1} \text{ s}^{-1}$ is shown for clarity as well. Fig. 3 shows the temperature dependence of conductivities of 2DHG in DS-MOD and SS-MOD samples obtained from the mobility spectrum analysis and the averaged conductivity of the whole heterostructures obtained from the standard resistivity measurements. At room-temperature, about 65% and 60% of the conductivity in DS-MOD and SS-MOD, respectively, originate from the parallel conduction. However, with reduction of temperature the conductivity of parallel layers decreases due to the carrier freeze-out, and below certain temperatures (100 K for DS-MOD and 20 K for SS-MOD), the parallel conduction disappears and 2DHG conductivity obtained from the mobility spectra analysis coincides with the conductivity obtained by the conventional resistivity measurements.

Due to the modification of the Ge QW valence energy band profile from the triangular-like of the SS-MOD to the rectangular-like of the DS-MOD, the room- and low-temperature 2DHG carrier densities in DS-MOD are increased by ~ 3.3 times and ~ 1.7 times, respectively, with respect to those in SS-MOD. The 2DHG density of DS-MOD at room-temperature is only $\sim 10\%$ lower than that at 10 K. This implies that it is the mobility enhancement with the reduction of the temperature that is responsible for the dramatic enhancement of 2DHG conductivity in DS-MOD at low temperatures.

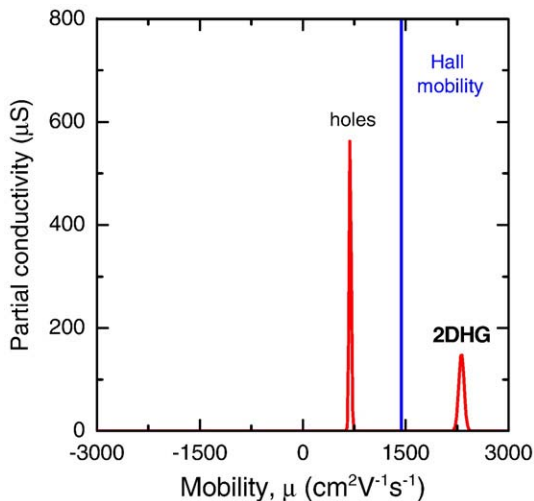


Fig. 2. Room-temperature mobility spectrum as the result of $\sigma_{xx}(B)$ and $\sigma_{xy}(B)$ fits for DS-MOD Ge QW heterostructure. The measured Hall mobility is shown for clarity.

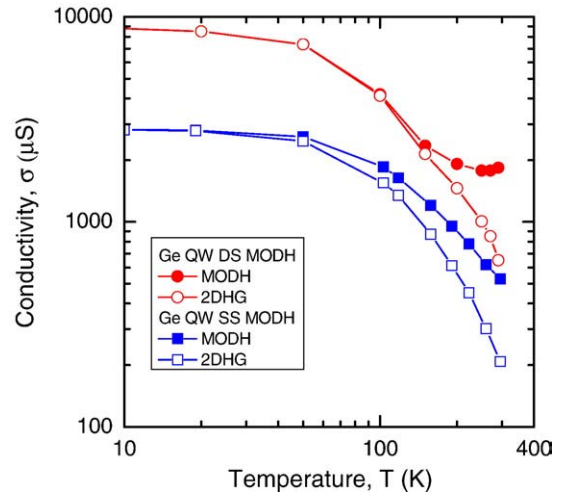


Fig. 3. The temperature dependence of conductivities of 2DHG in DS-MOD (open circles) and in SS-MOD (open squares) samples obtained by the mobility spectrum analysis and the temperature dependence of the averaged conductivity of the whole heterostructures for DS-MOD (filled circles) and in SS-MOD (filled squares) samples obtained from the standard resistivity measurements.

As expected, both the drift and Hall mobilities of carriers in DS-MOD and SS-MOD increase with decreasing temperatures. The 2DHG drift mobilities for both samples are higher than the Hall mobilities in the higher temperature range and they become equal below a certain temperature when the parallel conduction disappears. The 2DHG drift mobility of $30,000 \text{ cm}^2 \text{ V}^{-1} \text{ s}^{-1}$ in DS-MOD at low temperatures is a factor of two higher than that in SS-MOD. However, the 2DHG drift mobilities at room-temperature are about the same for both samples; $2380 \text{ cm}^2 \text{ V}^{-1} \text{ s}^{-1}$ for DS-MOD and $2540 \text{ cm}^2 \text{ V}^{-1} \text{ s}^{-1}$ for SS-MOD. The temperature dependence of the drift mobility in the high temperature region, 200–295 K, can be fitted very well using an empirical relation of $\mu \sim T^{-\alpha}$, with $\alpha = 1.57$ and 1.42 for DS-MOD and SS-MOD, respectively. The power-law behaviour with $\alpha \geq 2$ is established for the mobility limited by dominating phonon scattering in bulk Si and Ge [9], and $\alpha \approx 1.6$ obtained here is likely to represent the 2DHG drift mobility, in 8 nm compressive strained Ge QW, limited by phonon scattering. The small difference

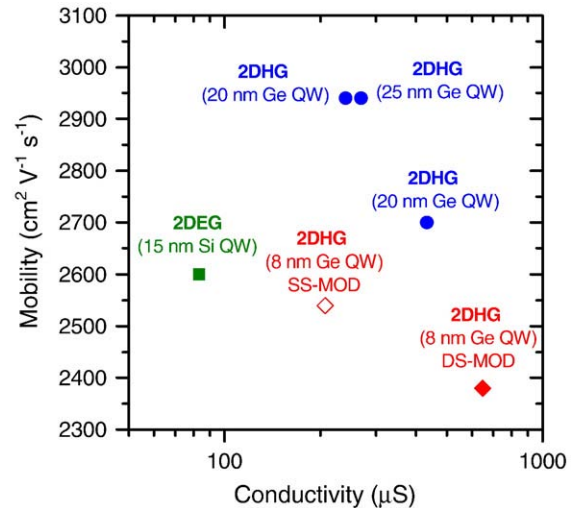


Fig. 4. The 2DHG and 2DEG drift mobilities as functions of the conductivity at room temperature. The 2DHG in SS-MOD 20 and 25 nm Ge QWs from Refs. [1,2,5,12] are shown by circles. The 2DEG in SS-MOD 10 nm Si QW from Ref. [11] is shown by square. The 2DHG in SS-MOD and DS-MOD 8 nm Ge QWs obtained in this work are shown by open and filled diamonds, respectively.

between $\alpha=1.42$ and 1.57 arises from the reduction of interface-roughness scattering in DS-MOD compared to SS-MOD. The mobilities limited by acoustic- and optical-phonon scatterings are known to be proportional to the width of the QW [10]. Therefore, further enhancement of the 2DHG mobility at room-temperature can be achieved in the future by increasing the width of Ge QW. This conclusion is in good agreement with previously reported results [6].

Fig. 4 shows 2DHG and 2DEG drift mobilities as functions of the conductivity at room-temperature. The highest values for previously published mobilities of 2DHG in strained Ge QWs, grown by various approaches, and 2DEG in the strained Si QWs along with the results obtained in this work are shown. For the highest published 2DEG mobility of $2830 \text{ cm}^2 \text{ V}^{-1} \text{ s}^{-1}$ neither carrier density nor conductivity was reported [11]. Anyway, it is clearly seen that the highest 2DHG mobility obtained in the SS-MOD strained 20–25 nm Ge QWs exceeds 2DEG ones obtained in the strained 10 nm Si QWs and many times higher than hole and electron mobilities in bulk Si at room-temperature. At the same time, the high 2DHG mobilities are obtained at much higher densities. By just implementation of DS-MOD with Ge QW of the same thickness, of 8 nm, the significant enhancement of 2DHG conductivity was obtained, which exceeds the previously reported conductivities of high mobility 2DEG and 2DHG. This demonstrates that p-type strained Ge QW channel have much higher conductivity than n-type strained Si QW channel.

In conclusion, over three times enhancement of room-temperature 2DHG conductivity up to $649.3 \mu\text{S}$ was obtained by implementation of DS-MOD with strained Ge QW of the same thickness. Such improvement was achieved by successful increase of the 2DHG density in the QW. The obtained 2DHG conductivity exceeds the previously reported high mobility 2DEG and 2DHG ones. These results open the possibility

for realization not only of future high performance symmetrical CMOS with strained p-Ge and n-Si channels on Si(001) or SOI(001) substrates but also high performance p-Ge channel FET devices for RF applications.

Acknowledgments

This work was supported by “High-Tech Research Center” Project for Private Universities; matching fund subsidy from MEXT, 2002–2007 and JSPS funding for young researchers 18760019.

References

- [1] M. Myronov, T. Irisawa, O.A. Mironov, S. Koh, Y. Shiraki, T.E. Whall, E.H.C. Parker, *Appl. Phys. Lett.* 80 (2002) 3117.
- [2] H. von Kanel, M. Kummer, G. Isella, E. Muller, T. Hackbarth, *Appl. Phys. Lett.* 80 (2002) 2922.
- [3] B. Rossner, D. Chrastina, G. Isella, H. von Kanel, *Appl. Phys. Lett.* 84 (2004) 3058.
- [4] M. Myronov, C.P. Parry, O.A. Mironov, E.H.C. Parker, *Appl. Phys. Lett.* 85 (2004) 3145.
- [5] R.J.H. Morris, T.J. Grasby, R. Hammond, M. Myronov, O.A. Mironov, D.R. Leadley, T.E. Whall, E.H.C. Parker, M.T. Currie, C.W. Leitz, E.A. Fitzgerald, *Semicond. Sci. Technol.* 19 (2004) L106.
- [6] M. Myronov, T. Irisawa, S. Koh, O.A. Mironov, T.E. Whall, E.H.C. Parker, Y. Shiraki, *J. Appl. Phys.* 97 (2005) 083701.
- [7] S. Kiatgamolchai, M. Myronov, O.A. Mironov, V.G. Kantser, E.H.C. Parker, T.E. Whall, *Phys. Rev. E* 66 (2002) art. no.
- [8] M. Myronov, K. Sawano, Y. Shiraki, *Appl. Phys. Lett.* 88 (2006) art. no.
- [9] S.M. Sze, *Physics of semiconductor devices*, Wiley, New York; Chichester, 1981.
- [10] B. Laikhtman, R.A. Kiehl, *Phys. Rev. B-Condens Matter* 47 (1993) 10515.
- [11] S.F. Nelson, K. Ismail, J.O. Chu, B.S. Meyerson, *Appl. Phys. Lett.* 63 (1993) 367.
- [12] H. von Kanel, D. Chrastina, B. Rossner, G. Isella, J.P. Hague, M. Bollani, *Microelectron. Eng.* 76 (2004) 279.